Examples

M.Theiss Hard- and Software for Optical Spectroscopy
Dr.-Bernhard-Klein-Str. 110, D-52078 Aachen
Phone: (49) 241 5661390   Fax: (49) 241 9529100
E-mail: theiss@mtheiss.com   Web: www.mtheiss.com
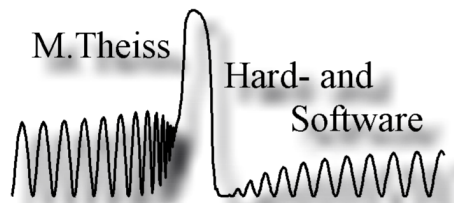
SPRAY

Spectral ray-tracing simulations

by Wolfgang Theiss

Printed: 01.12.2009, 22:52 in Aachen, Germany

Table of Contents

Part

I

1   Introduction

1.1   About this document

Spectral Ray Tracing

Examples

© W.Theiss

M. Theiss – Hard- and Software
Dr.-Bernhard-Klein-Str. 110, D-52078 Aachen, Germany
Phone: + 49 241 5661390   Fax: + 49 241 9529100
e-mail: theiss@mtheiss.com   web: www.mtheiss.com

September 2001

1.2   Overview

This document describes introductory examples demonstrating important SPRAY features. The SPRAY manual should be consulted for details of the individual objects.

Chromatic error of a collecting lens
Collecting lens: edge effects
An IR reflectance unit for variable angle of incidence
Dipole scattering - blue skies and red sunsets
Paints: Beyond Kubelka-Munk

Part

II
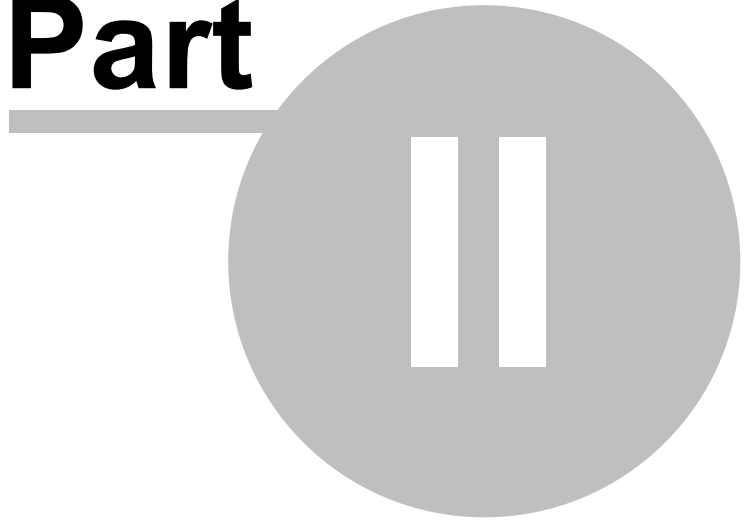
2 Lenses

2.1 Chromatic error

SPRAY is used to investigate the shift of the focal plane of a collecting lens with wavelength.

A circular light source (left) creates a parallel beam which is focussed by a collecting lens (right):

Sending some test rays the function of the lens is demonstrated:
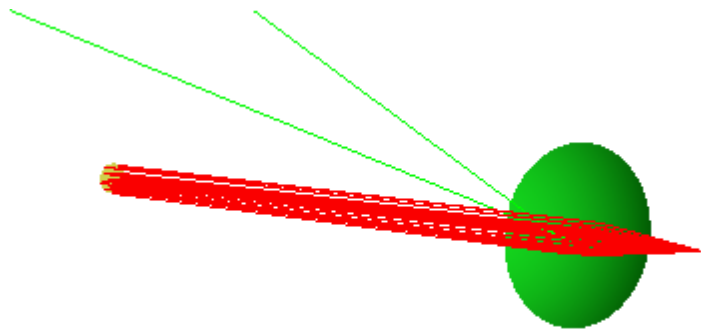
In the focal plane of the lens an array detector (length: 3 mm, 30 pixels) is placed which records position-dependent spectra along the symmetry axis of the system:
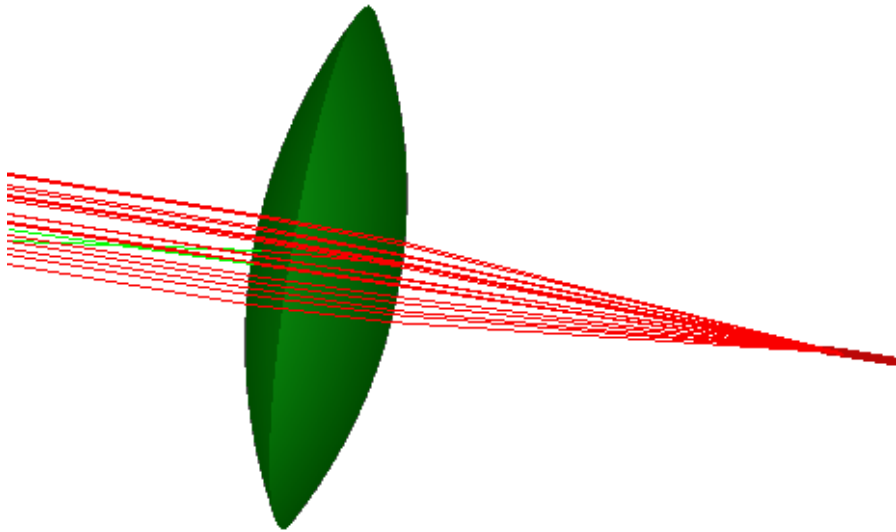
If the optical constants of BK7 glass are used for the lens the following intensity distribution is observed:
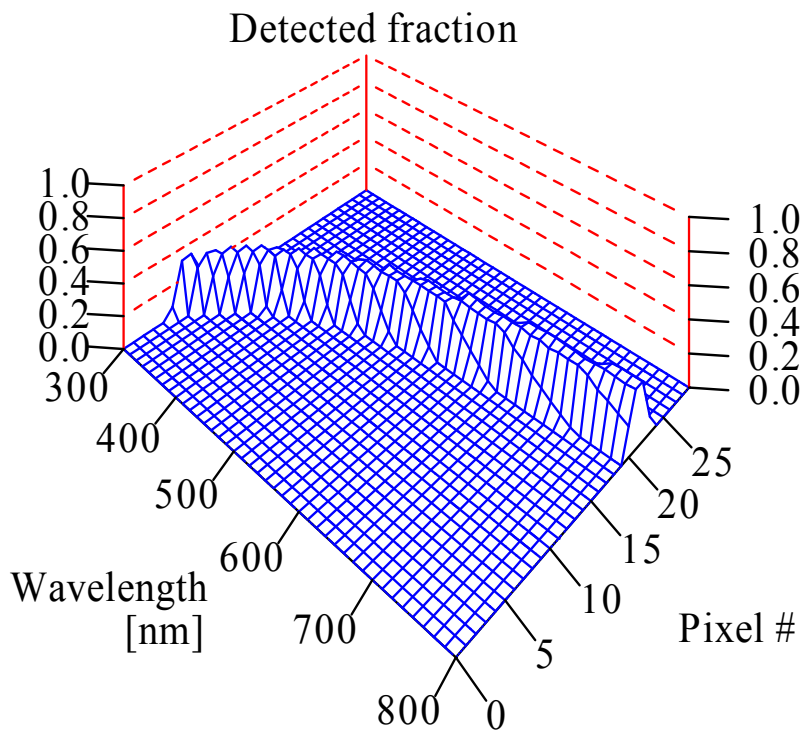
Clearly blue light (400 nm) is focussed closer to the lens than red light (700 nm) which is due to the dispersion of the glass. The refractive index of BK7 has the following spectral dependence:

BK7
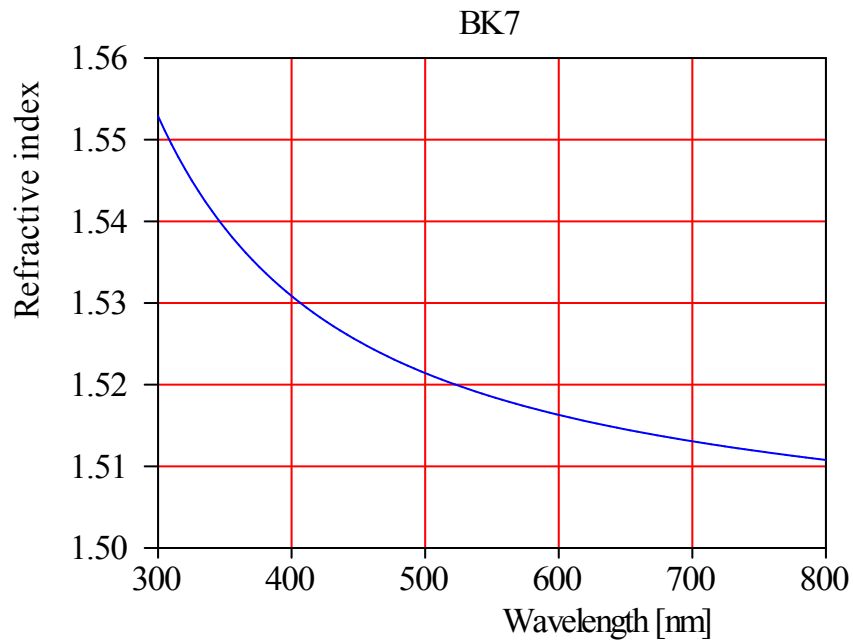
2.2 Edge effects

The imaging quality of a simple lens decreases with the distance of incoming rays from the center of the lens. The configuration previously used to demonstrate chromatic errors is used here to show how the size of the focus depends on the diameter of the incoming beam.

Setting the beam diameter to 0.2 cm (i.e. the radius of the circular light source to 0.1 cm) a very sharp focus is achieved. As shown before, the position of the focal plane depends on wavelength due to the dispersion of the optical constants of the glass:
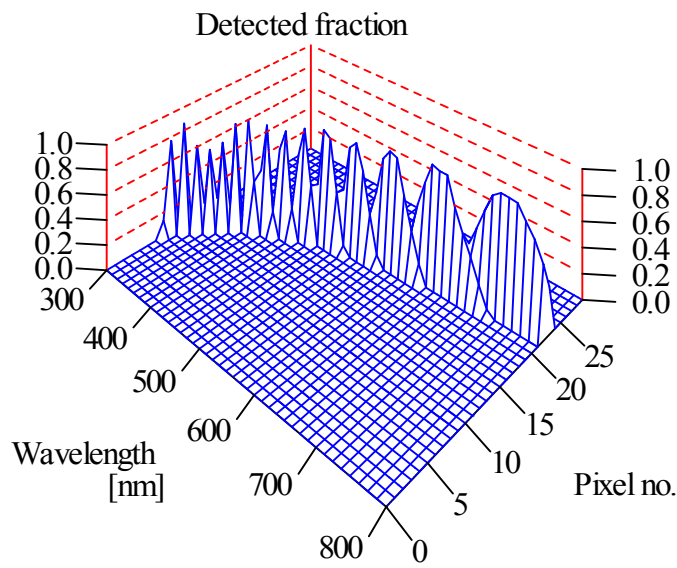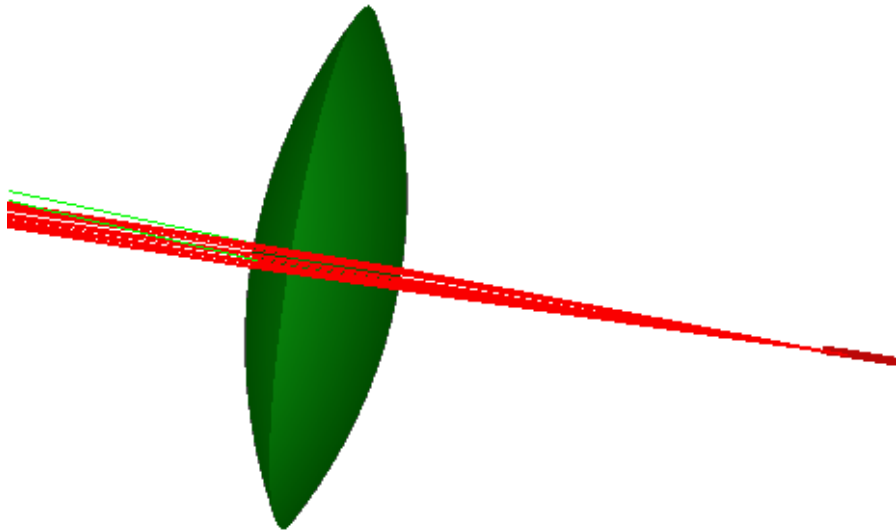
Increasing the beam diameter to 0.6 cm a much larger portion of the lens is used to collect light:
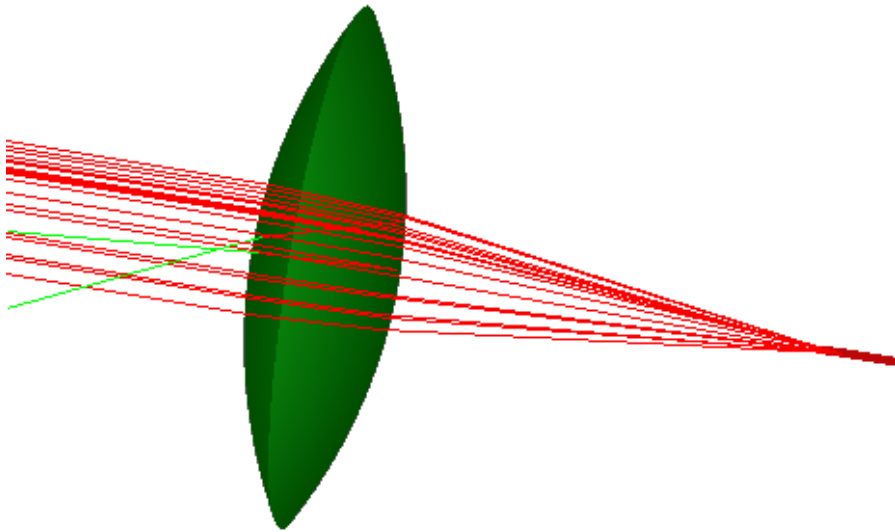
However, now the focus is much broader:
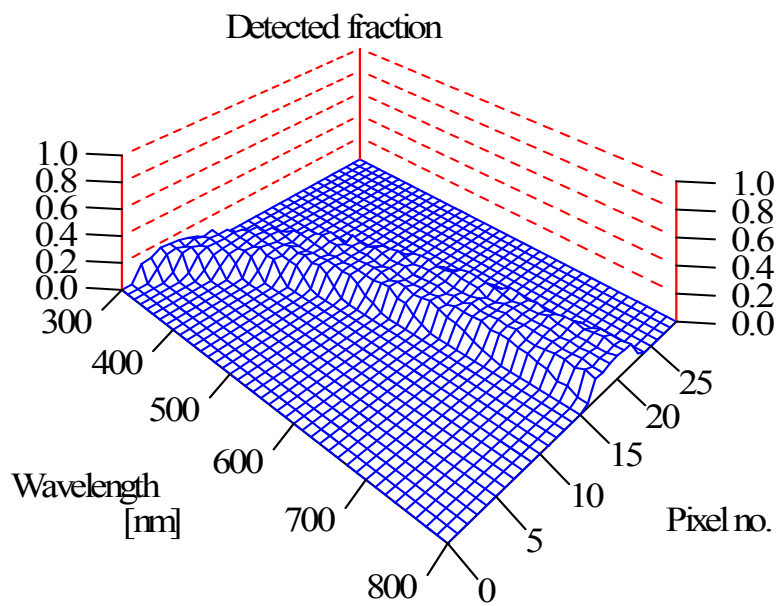
Blocking the rays in the center of the beam with a circular stop of 0.4 cm diameter
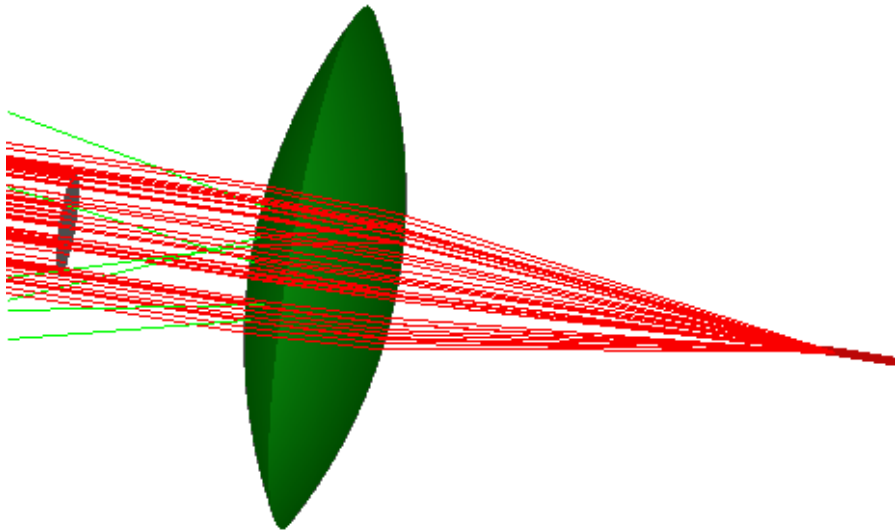
makes clear that the rays at the outer regions of the lens are focussed in a different plane as those that hit the lens in the center (see figure above):

Part

III
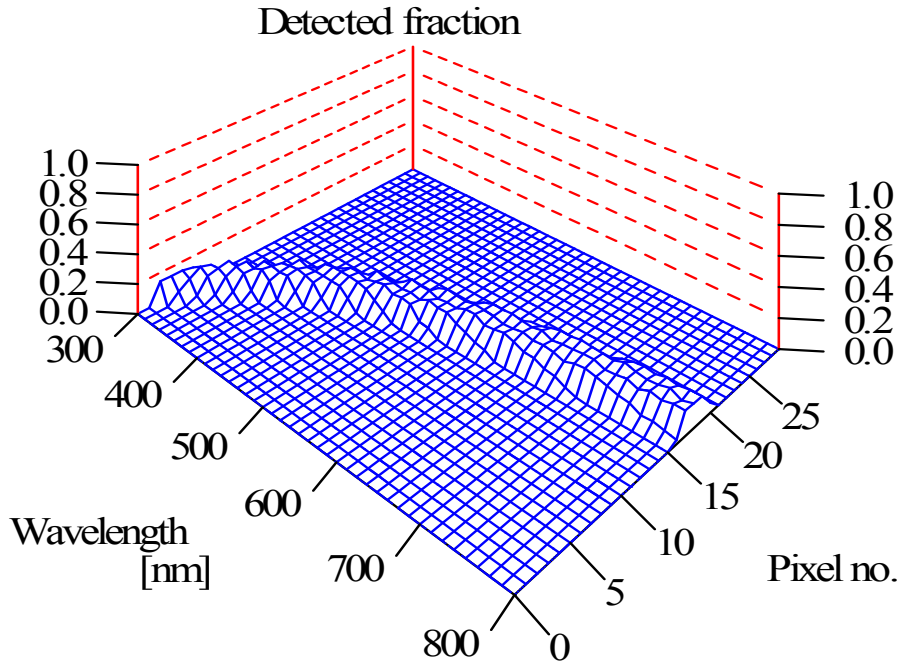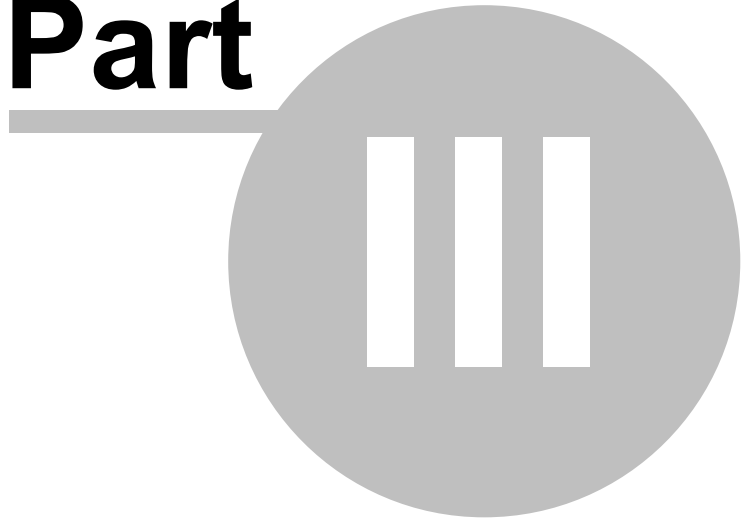
3   IR reflectance unit

3.1   Overview

This section demonstrates the simulation of an almost realistic reflectance unit. Devices like this are often used in the sample compartment of infrared spectrometers in order to record reflectance spectra of samples at various angles of incidence and different polarizations.

The SPRAY setup includes the following items: A circular light source emits divergent radiation directed towards a parabolic mirror. The light source is placed in the focus of the paraboloid - hence a parallel beam is created by the mirror. A second parabolic mirror creates a focus on a rotatable plane mirror.

In real spectrometers a Michelson interferometer - consisting of a beam splitter and a fixed and movable plane mirror - is usually placed between the two paraboloids. The interferometer is skipped in this setup because the performance of the reflectance unit is of interest here.

The plane mirror directs the radiation upwards onto an elliptical mirror. The center of the rotatable mirror as well as the sample position are the focal points of the ellipsoid. A second ellipsoid directs the beam reflected by the sample (here a perfect plane mirror is taken as sample) towards a second rotatable mirror. Finally the beam is focussed by another ellipsoidal mirror to the detector element which records the spectrum.

Here is a side view of the setup (with and without some test rays sent to visualize the function of the elements):
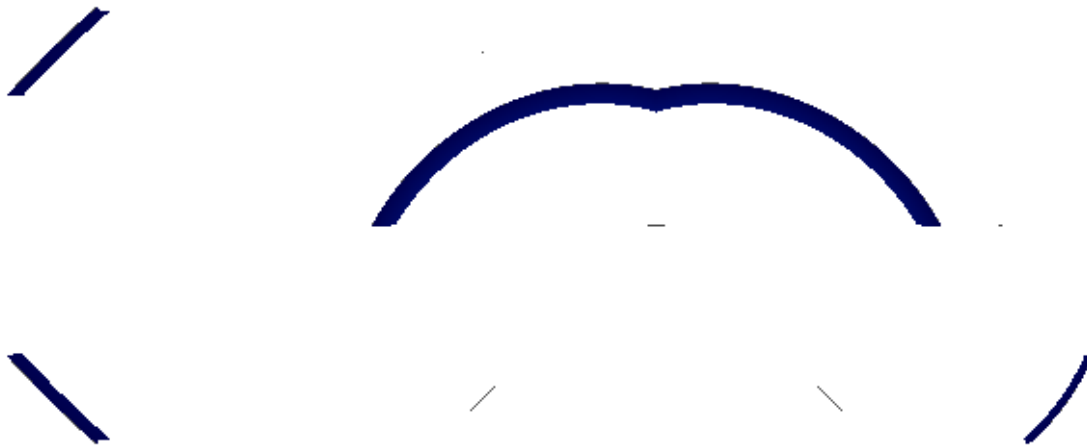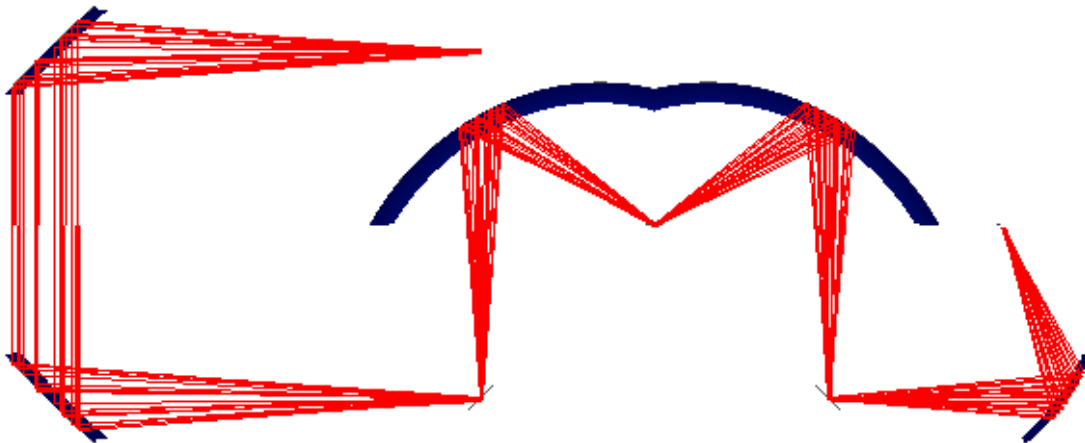
Viewed from the top the scenery looks like this:
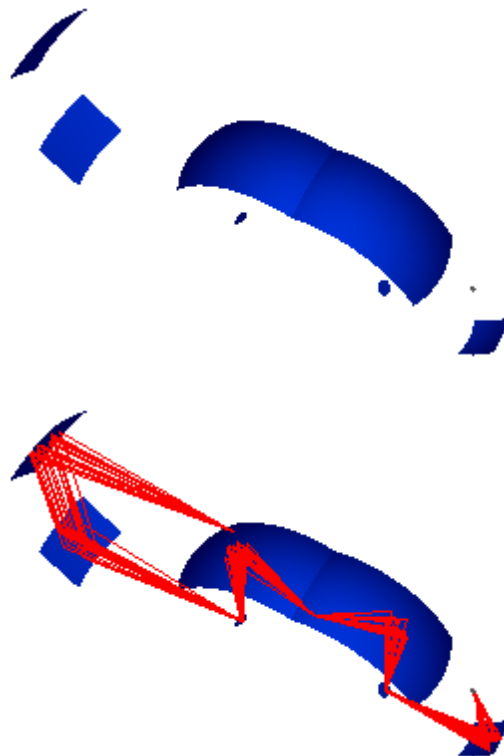
3.2   Spot size vs. angle of incidence

In some analytical problems the size of available samples is limited and you have to know how large the illuminated sample spot is. Placing a screen slightly above the sample position is the easiest way to visualize the illuminated sample area.

The following pictures show the intensity distribution on a quadratic screen (10 mm by 10 mm)

for different rotation angles of the   rotatable mirrors. First almost normal incidence of light is taken:
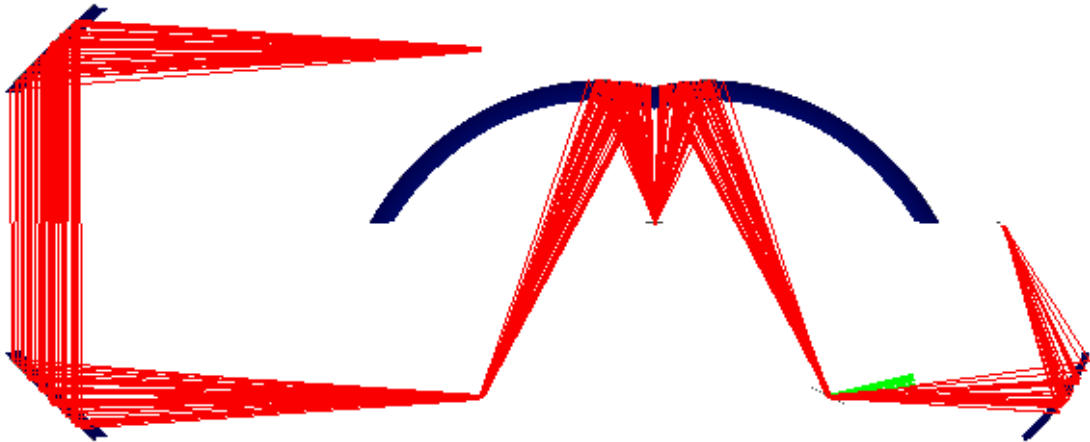
An almost circular spot of about 2 mm diameter is found:
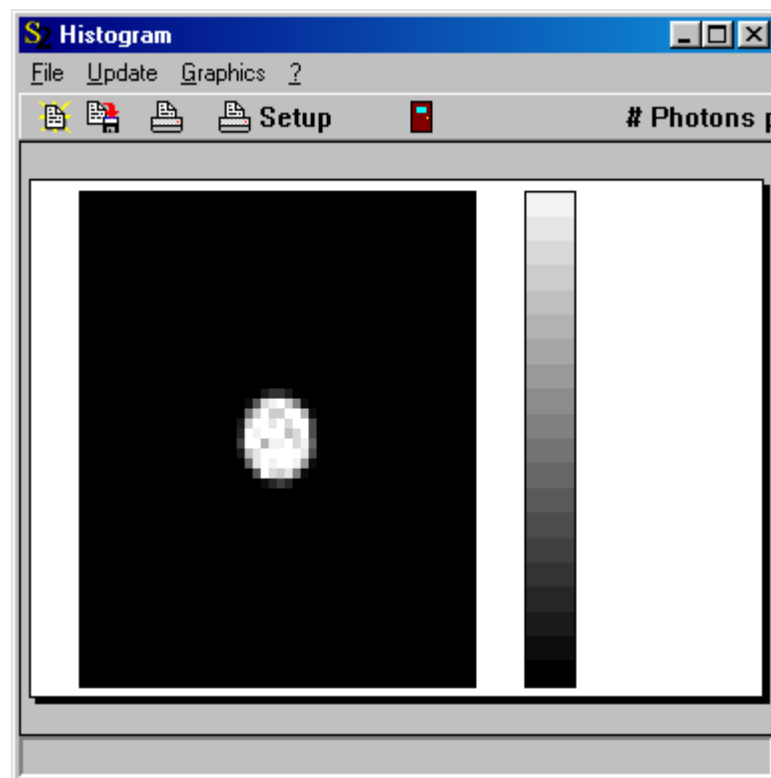
For larger angles of incidence the spot broadens:
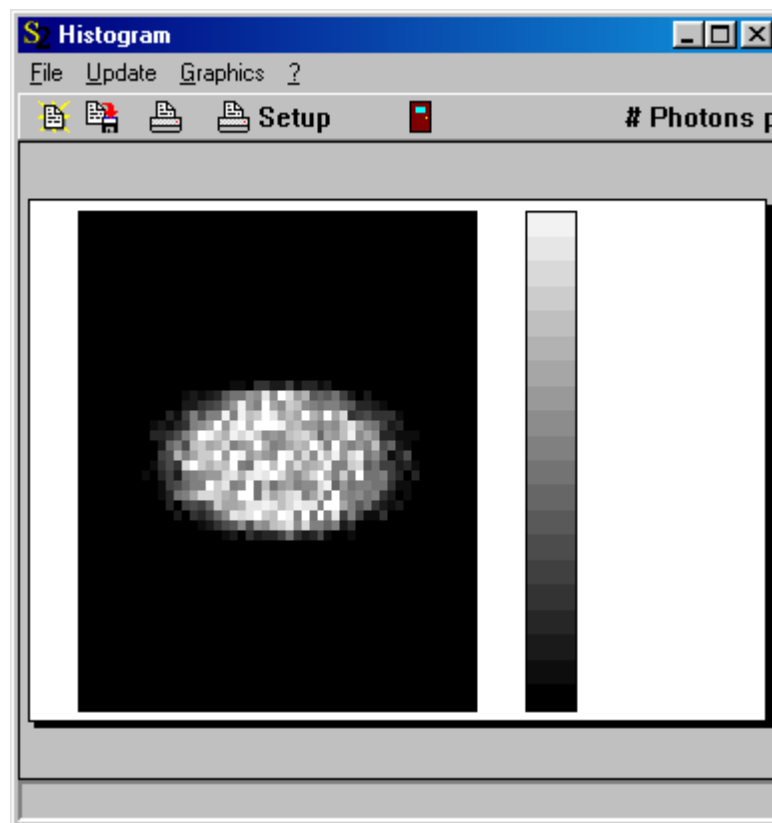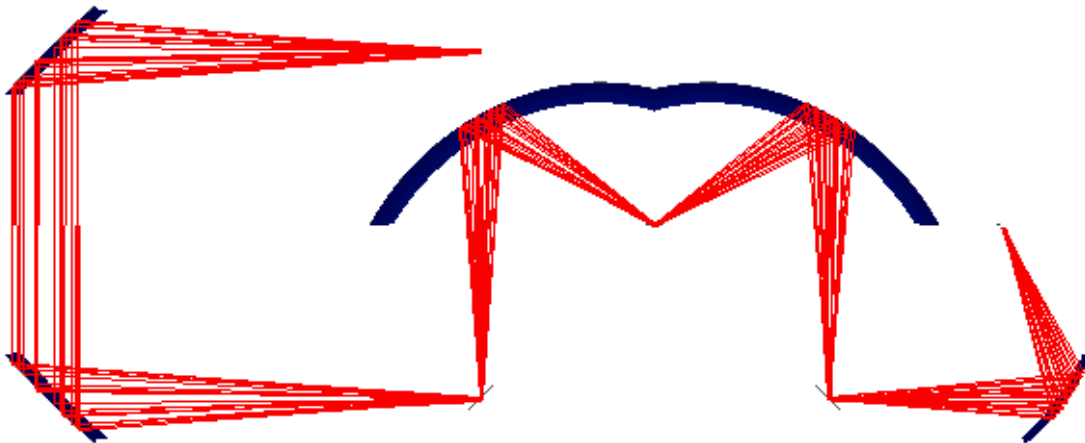
For extremely large angles of incidence the spot gets even larger than the screen:
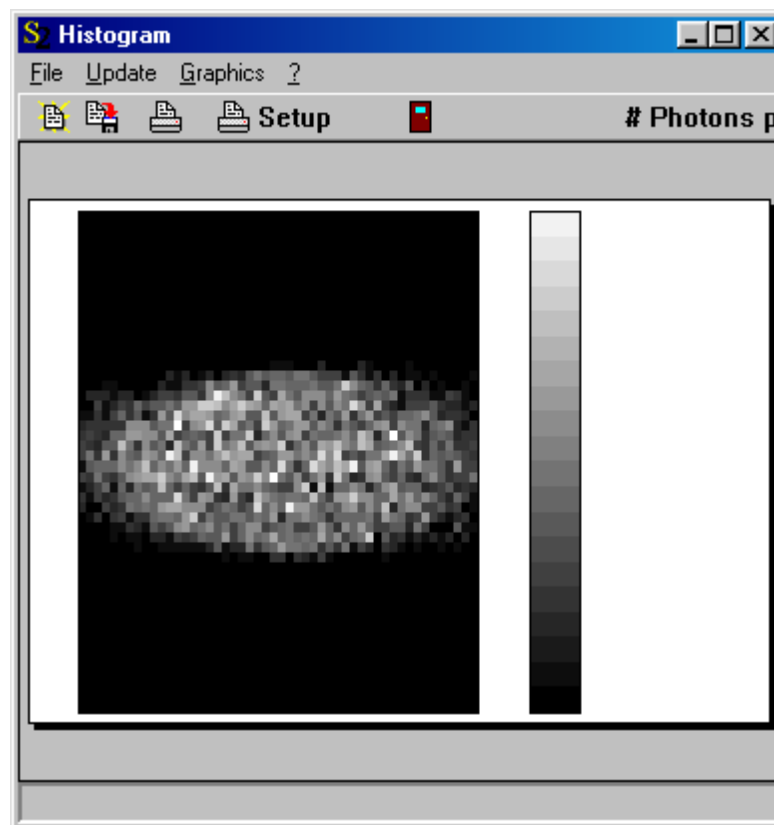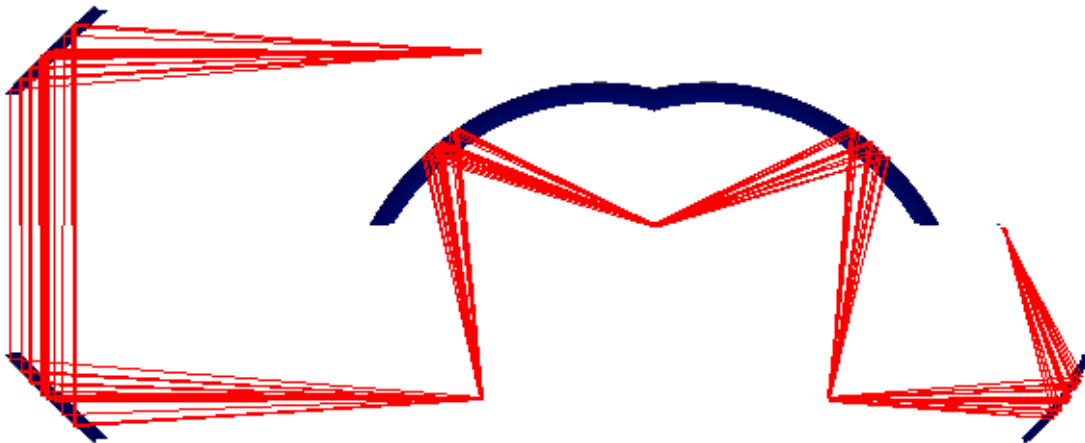
3.3   Alignment sensitivity

Optical setups are not always perfectly aligned, and it may be of interest how variations of some geometrical parameters influence the performance of a device. SPRAY simulations can help to investigate misalignment effects. This is shown in the following simple example.

Ideal alignment leads to a throughput of the reflectance unit of 100% (ideal mirrors are assumed):
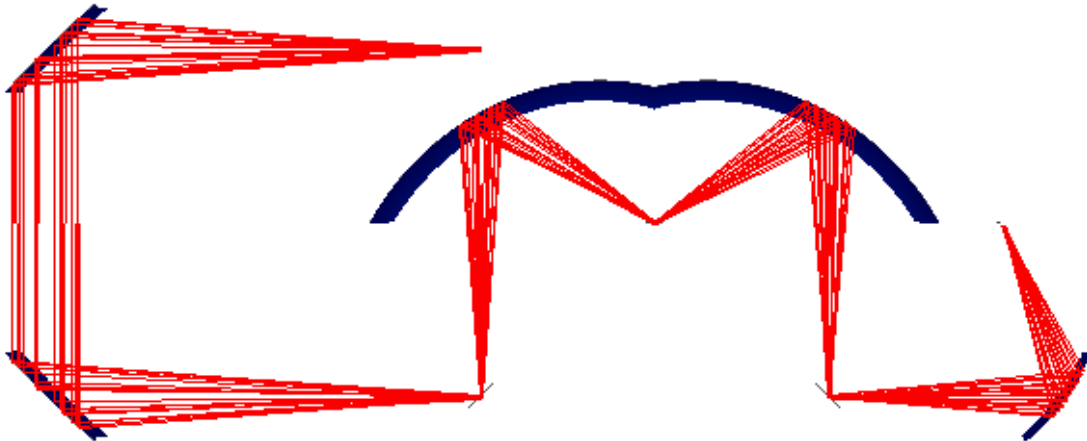
If the sample is moved up from its ideal position by 5 mm no rays reach the detector any more:
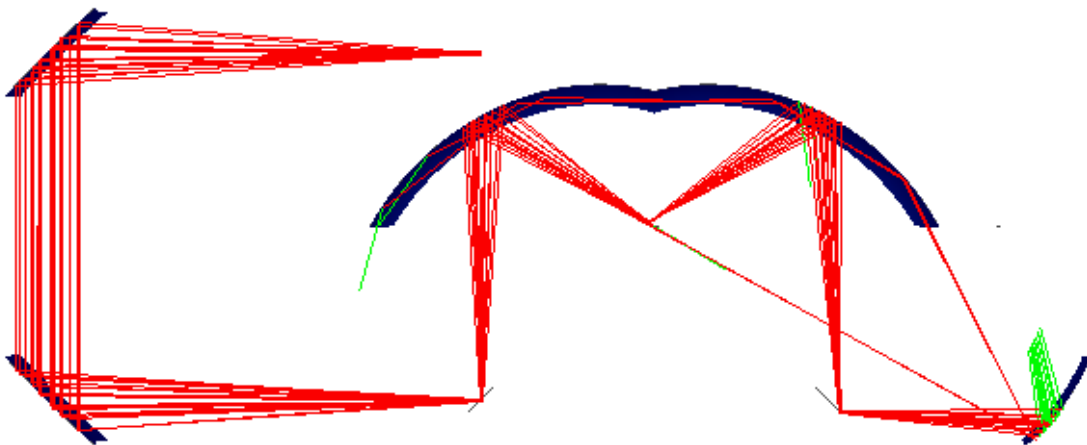
In order to investigate how the detector signal decreases with sample position many SPRAY simulations have to be performed. Using OLE automation the sample height can be automatically varied by an Excel macro, the detector signal is recorded and the following display of the detected fraction of rays vs. the z coordinate of the sample is generated:
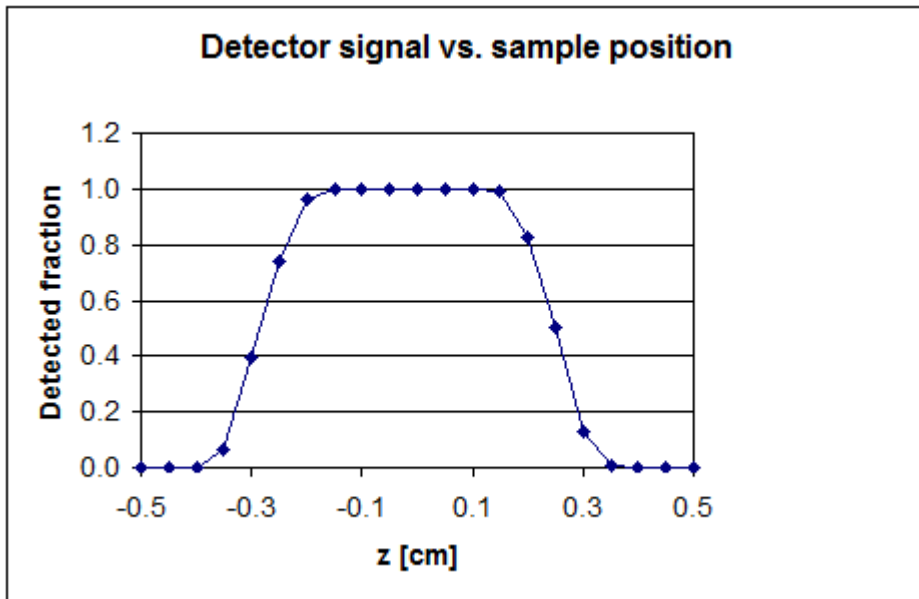
For almost normal incidence of light
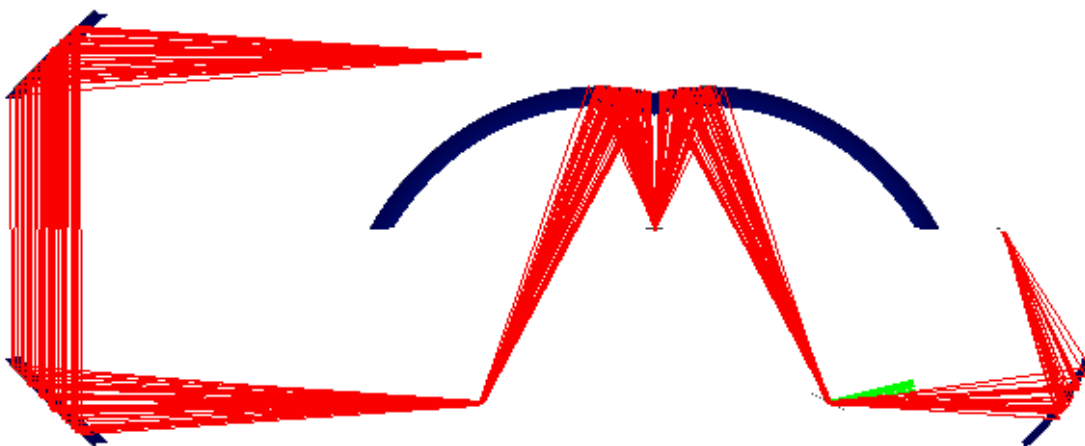
the z-alignment of the sample is significantly less critical:

Detector signal vs. sample position
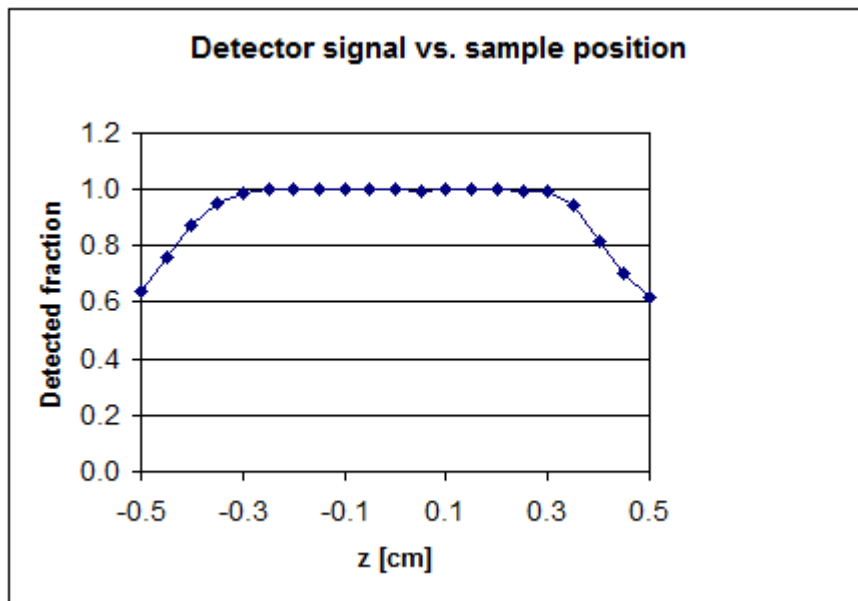
3.4   ATR experiment

Reflectance units like the one discussed here are often used in combination with ATR (attenuated total reflection). If a multiple reflection ATR crystal made of silicon is placed at the sample position the situation is this:
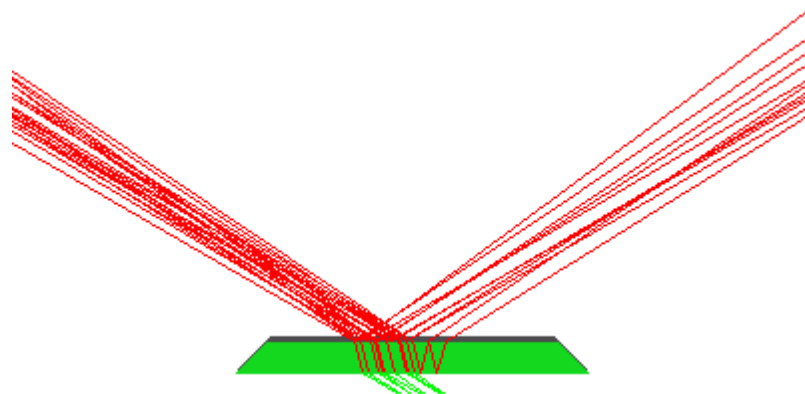
Here is a side view of the setup:
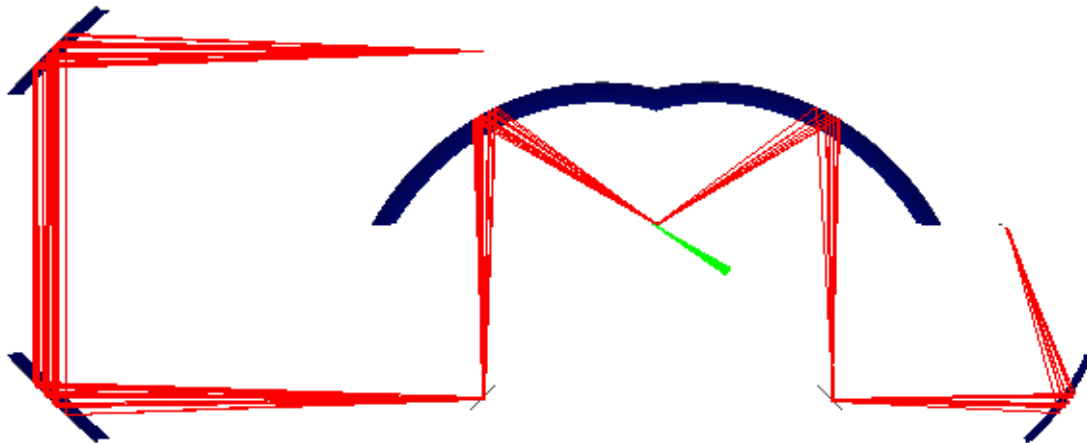
Obviously the ATR crystal has to be moved up in order to work properly because the radiation has to enter the crystal from the 45° edges. In order to find the best position we can let SPRAY do the work, controlled by OLE automation commands from Excel's VisualBasic in this case. Varying the height of the ATR element and recording the detector signals one gets the following results:
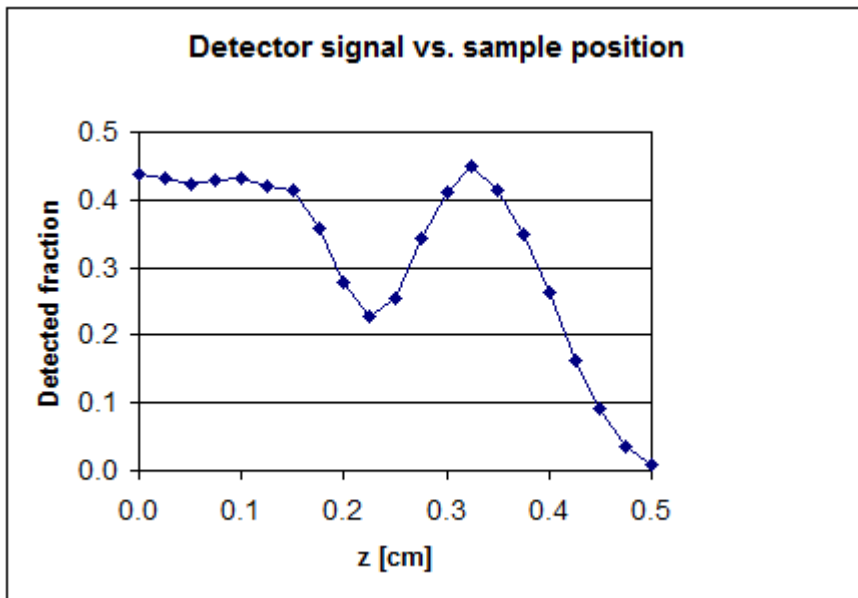
Trying a z-value of 0.33 seems to be promising. In fact, the light throughput is much better now:
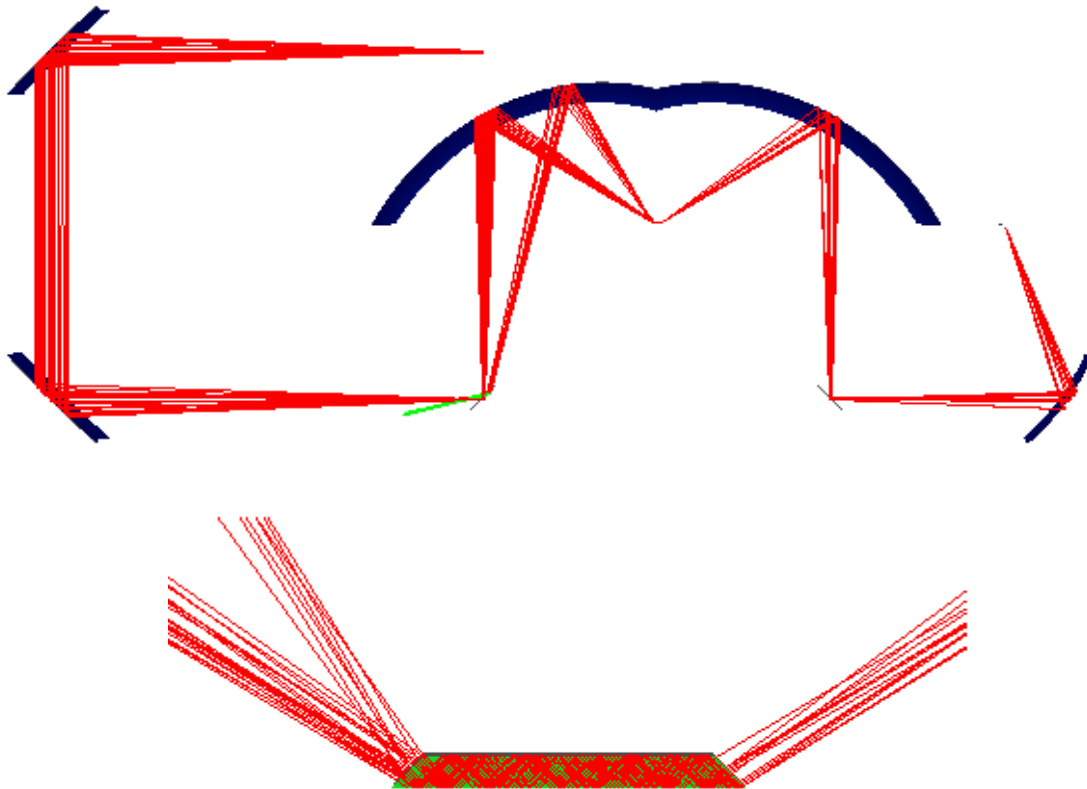
There are 5 total reflections at the bottom side of the ATR element on the average:
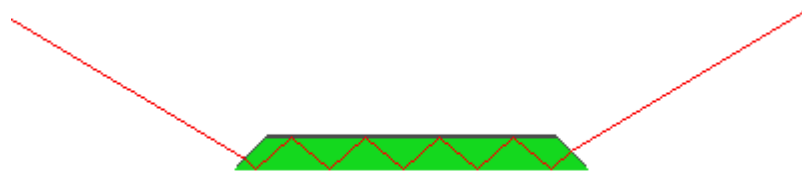
Part IV

4   Light scattering

4.1   Dipole scattering - blue skies and red sunsets

This is a simple example of light scattering effects studied with SPRAY. A parallel light beam (sun light) is directed into a region with very small particles - these particles represent density fluctuations in the earth's atmosphere which lead to dipole scattering. SPRAY determines how much light is received behind the scatterers and the fraction of rays scattered to the side. In both cases not only the spectra but also the corresponding colors are computed.

The required scattering properties are computed using an external small program that performs Mie computations (light scattering by spheres). Although water spheres have been used to generate the data, the results are quite universal since the spheres are so small that they have almost only dipole properties. The scattering characteristics (viewed with the tool view_rt.exe) are the following:
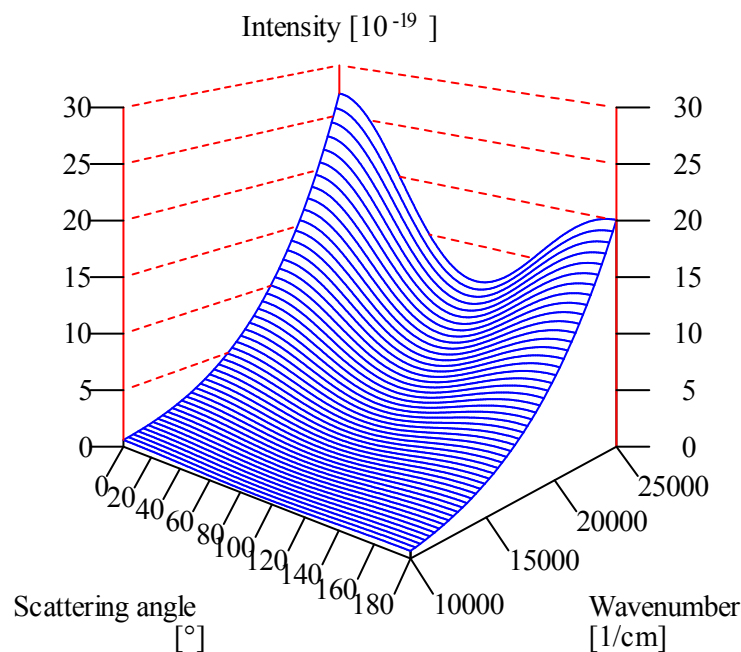
Setting the volume fraction of the scattering particles to 0.0001 one gets the following probabilities for scattering (red curve) and absorption (blue) per cm distance:

Absorption and scattering data
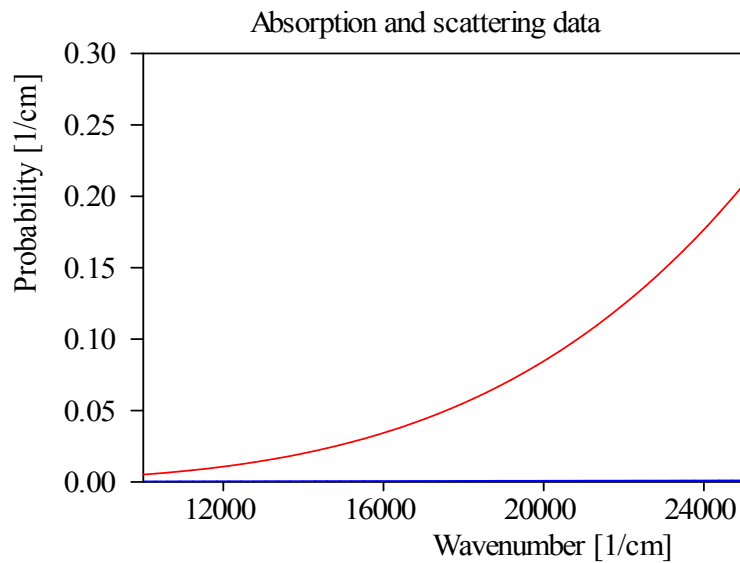
Clearly blue light (wavenumber 25000 1/cm, or 400 nm wavelength) is scattered more efficiently than red light (700 nm wavelength, corresponding to about 14000 1/cm). The consequences for the propagation of light through a volume filled with dipoles are investigated in a simple SPRAY configuration described in the following.

The parallel light beam created by a circular light source (left object in the picture below) is directed to a large sphere filled with the scattering dipoles (volume fraction: 0.0001). The rays transmitted straightahead through the scattering volume are recorded by the rectangular detector displayed to the right. The large detector in front is used to detect the radiation scattered sideways:
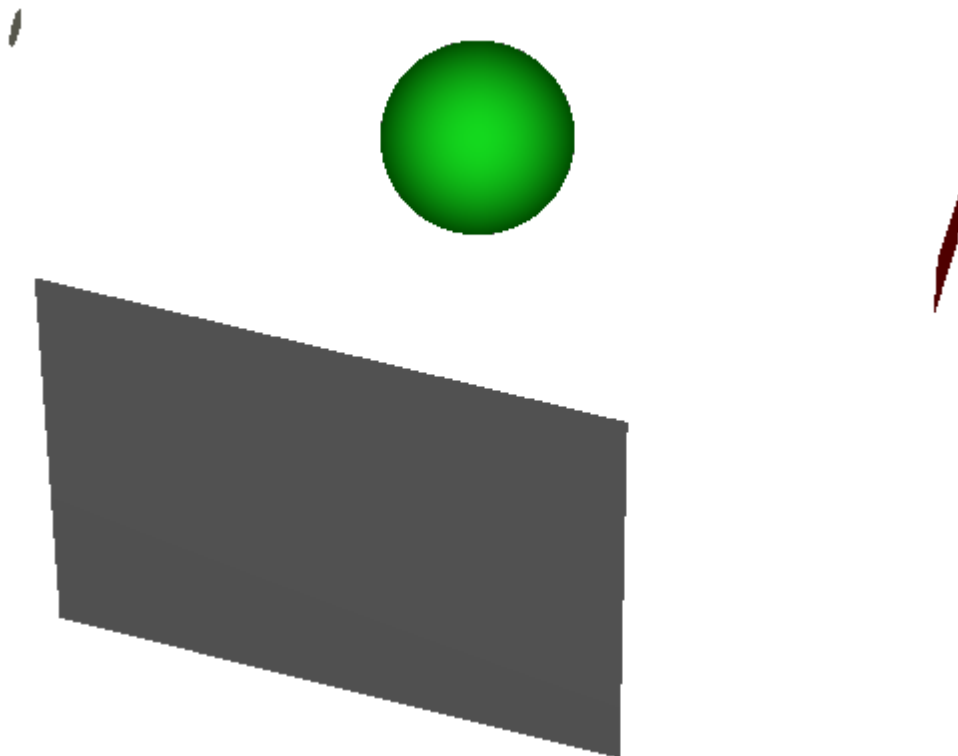
Testing the configuration with some rays (at 500 nm wavelength) gives a qualitative view of the effects:
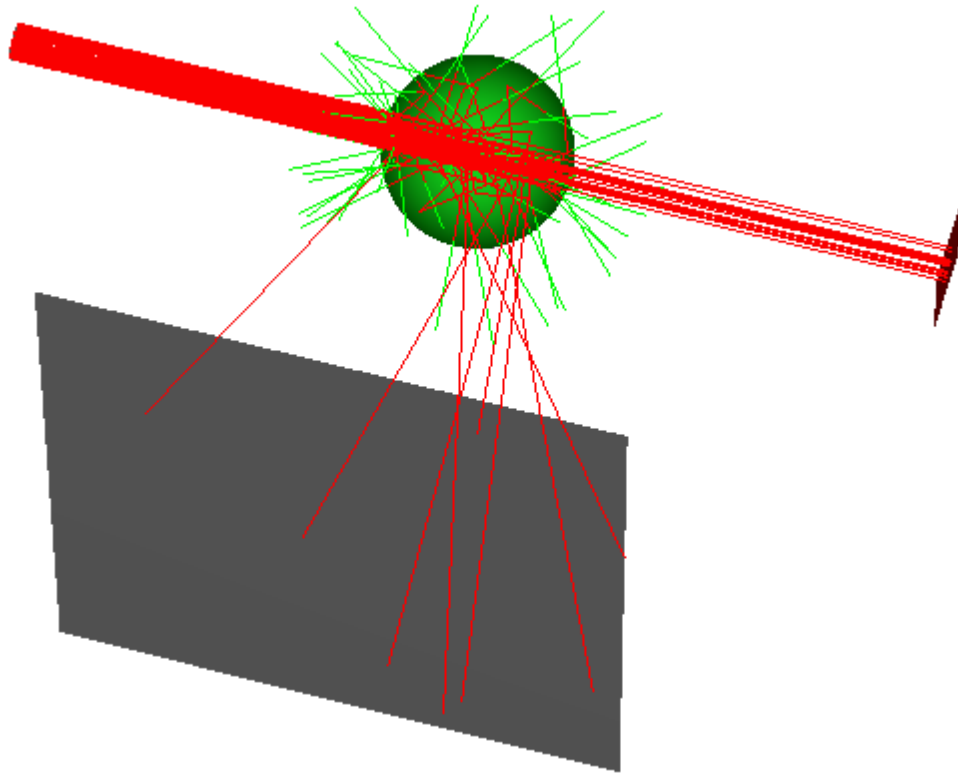
A certain fraction of the rays remains unscattered and reaches the 'throughput' detector, whereas the scattered fraction is distributed in all directions.

Doing the simulation with 41 spectral points in the range 400 ... 800 nm and 10000 rays per spectral point, the following results are obtained. The transmitted radiation has the following spectral distribution and color (which is computed by SPRAY as well):

'Throughput detector'
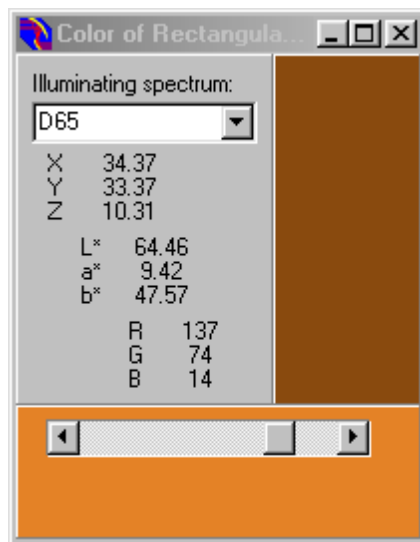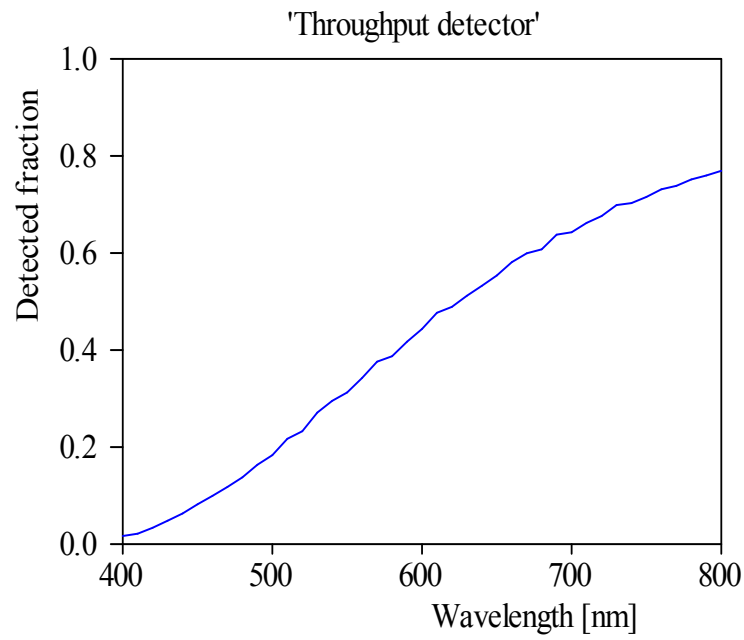
The missing rays in the blue are scattered to the side:

'Side detector'
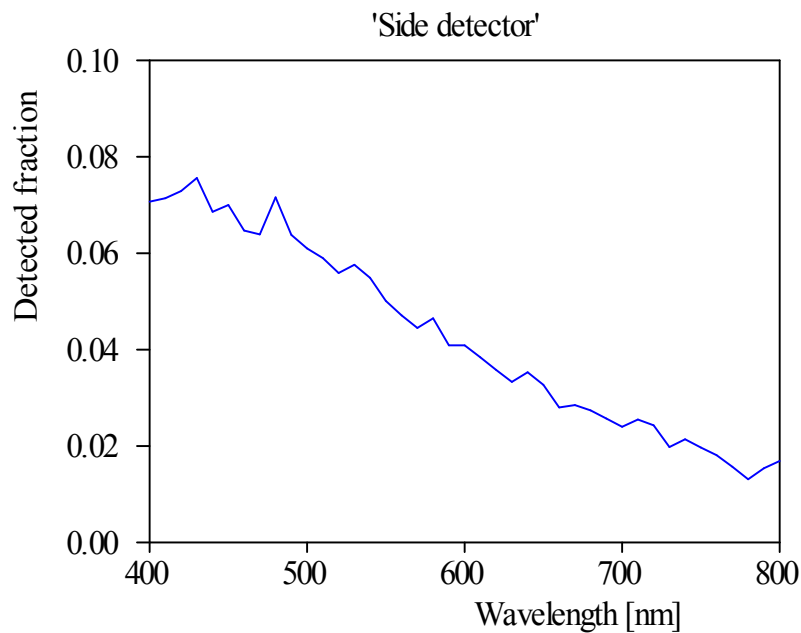
The conclusions from this simple simulation are the following: Light travelling through a medium filled with scattering dipoles looses blue light and appears to be red (like sunlight closely before sunset when it has to travel the largest distance through the earth's atmosphere). Watching light scattering dipoles from the side (that's what you do looking at the sky) gives a blue appearance.

4.2   Paints

4.2.1   Paints: Beyond Kubelka-Munk

This example shows how SPRAY can be used to predict colors of paints. In most cases paints consist of a transparent host material (resin) with embedded particles that scatter and absorb light. For the design of paints it is important to know how the amount of reflected light and its spectral composition depend on the concentrations and types of inclusions. Problems of this kind are often approached applying the so-called Kubelka-Munk theory. This rather old concept is a

two-flux radiation transfer model. In its simplest form it assumes diffuse illumination, isotropic scattering and perfect interfaces air-resin and resin-substrate. The probabilities per distance for absorption $K(\lambda)$ and scattering $S(\lambda)$ must be known - these are the input quantities of the model. The Kubelka-Munk theory returns the diffuse reflection coefficient of the paint for each wavelength.

Using SPRAY you can do the same - but with less approximations and much more realisitic results. The required input quantities are the scattering and absorption properties of each particle species, the optical constants of all materials involved and - of course - the geometry of the setup like the thickness of the resin or the direction of the incident radiation. You can increase the complexity of the model as you like - approaching more and more the real paint.

This SPRAY application example investigates a very simple model paint. Spherical inclusions are embedded in a resin with a constant and real refractive index of 1.5 - the resin itself does not absorb light. The following inclusions are used:

* Large TiO2 spheres
* Small TiO2 spheres
* Very small CdS spheres

The scattering and absorption properties of the inclusions are summarized in their individual sections (just double-click the links above).

The SPRAY configuration used to investigate the paint properties is described in the section 'The test system'. Before the actual work is done some short initial tests confirm the consistency of the setup.

The TiO2 spheres will be used to create diffuse light scattering almost independent of wavelength. In a first exercise we will learn how much inclusions we have to take in order to get a white paint covering a black substrate. The required amount strongly depends on the particle size. This is demonstrated comparing the case of large and small TiO2 spheres.

In a second step CdS clusters are added. They mainly function as absorbers in the blue and will be responsible for the color of the paint.

4.2.2   Scatterers

4.2.2.1   Large TiO2 spheres

The scattering properties of TiO2 spheres are computed using the external Mie program. The optical constants of TiO2 have been taken from the SPRAY database. In order to avoid some numerical problems of the Mie software, a small imaginary part has been added to the dielectric function which would be purely real otherwise.
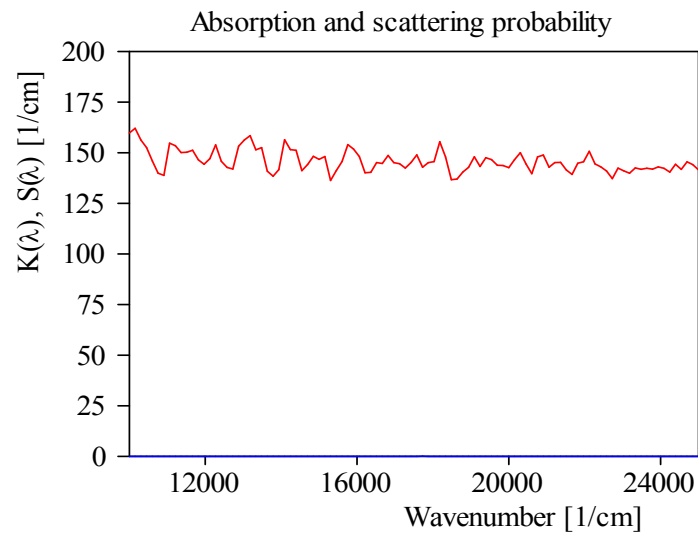The radius distribution for the Mie computation is this:

Size distribution large TiO2 spheres
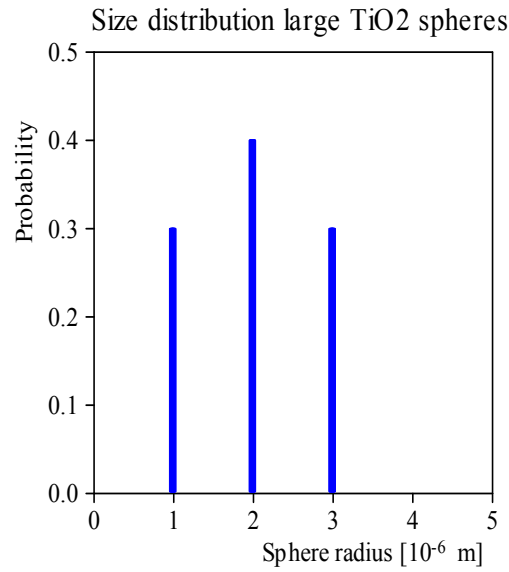
The spectral and angular distribution of the scattered intensity is dominated by forward and backward scattering
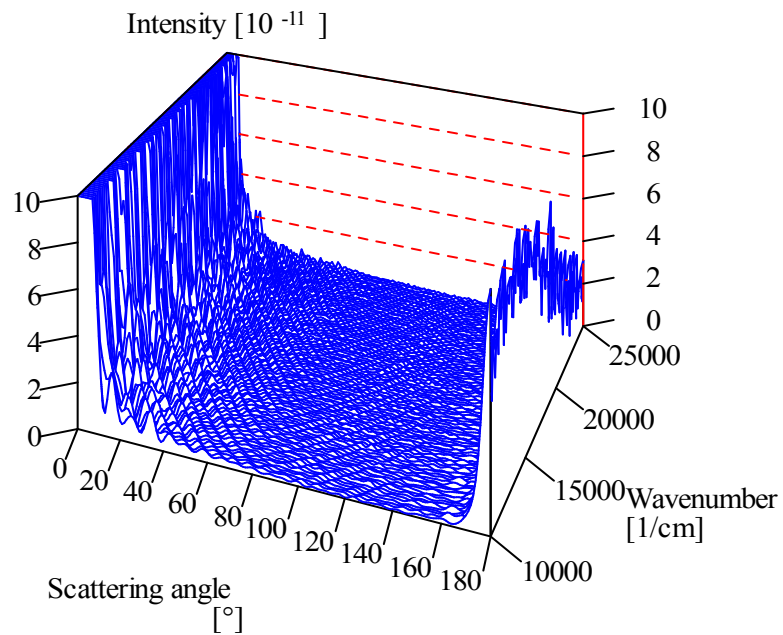

If these particles are embedded in the resin with a volume fraction of 1% one gets the following absorption (blue curve) and scattering probabilities/distance (red):
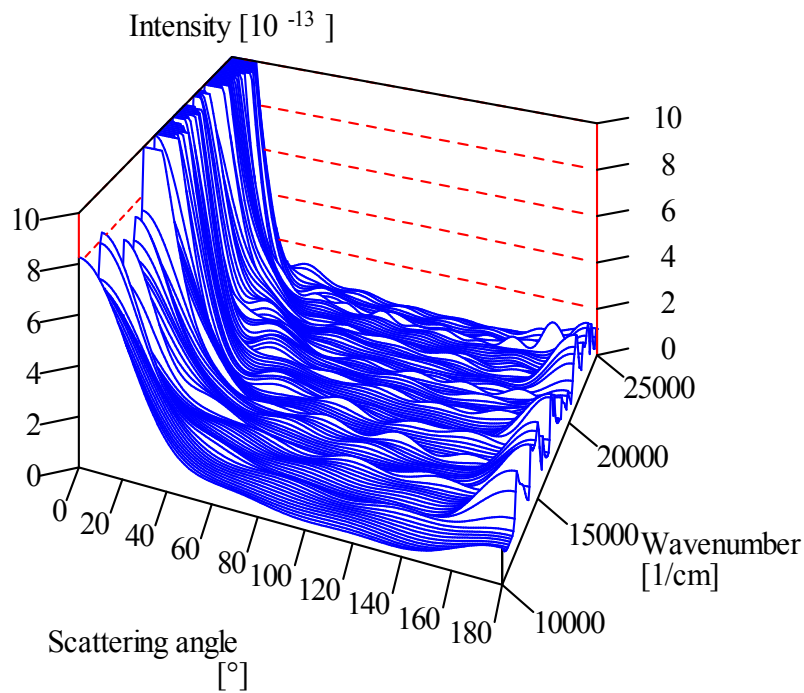
Absorption and scattering probability

changes the angular distribution of the scattered intensity significantly. There is still preferred forward and backward scattering but now the difference to the other directions is not so large any more:

In summary: The large TiO2 particles scatter light mainly in the forward direction. There is also pronounced backward scattering, but no absorption. All these properties are independent of wavelength.

4.2.2.2 Small TiO2 spheres

Reducing the size of the large TiO2 particles by a factor of 10
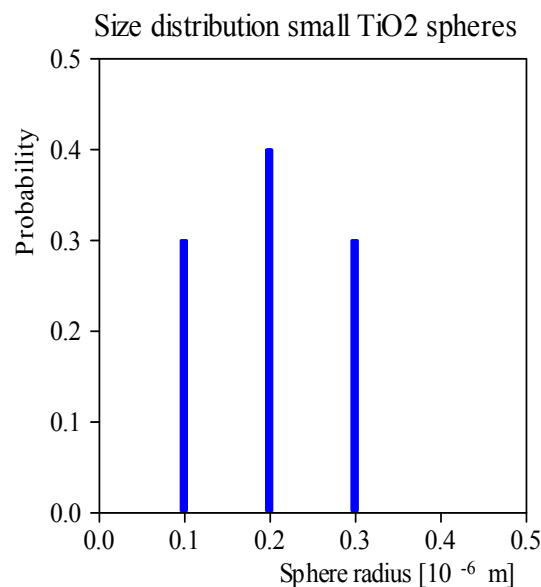
Size distribution small TiO2 spheres

Intensity [10 $^{-13}$]

Filling up the resin with these small TiO2 spheres (1% volume fraction) gives these scattering probabilities:

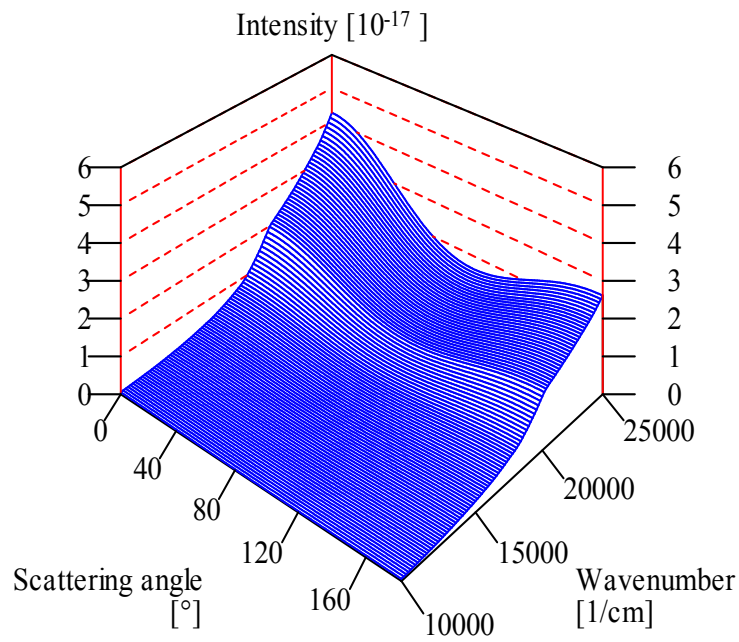Absorption and scattering probability
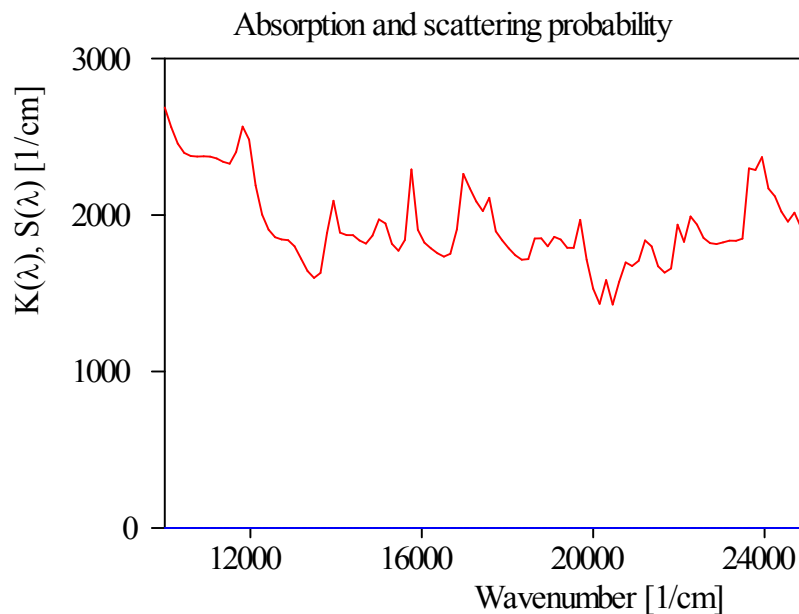
Note the much larger probability for scattering events compared to the large TiO2 spheres which is the main difference between the two types of TiO2 scatterers discussed here.

4.2.2.3   CdS clusters

The optical constants of the CdS clusters are taken from the SPRAY database. The radius distribution used in the Mie computation is shown below:

Size distribution CdS clusters
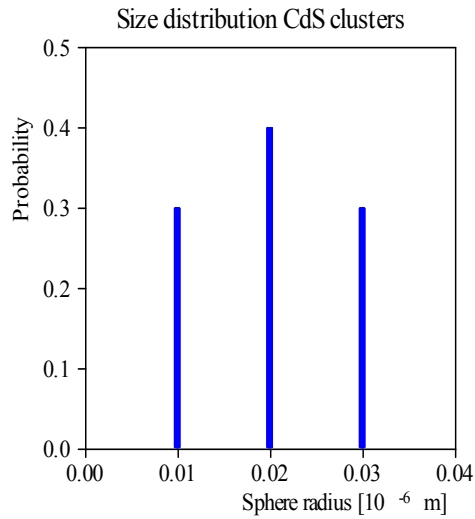
Due to the very small sizes the scattering is almost dipole scattering:

Intensity $[10^{-17}]$

The CdS particles in the resin (1% volume fraction) absorb and scatter with the following probabilities:

Absorption and scattering probability
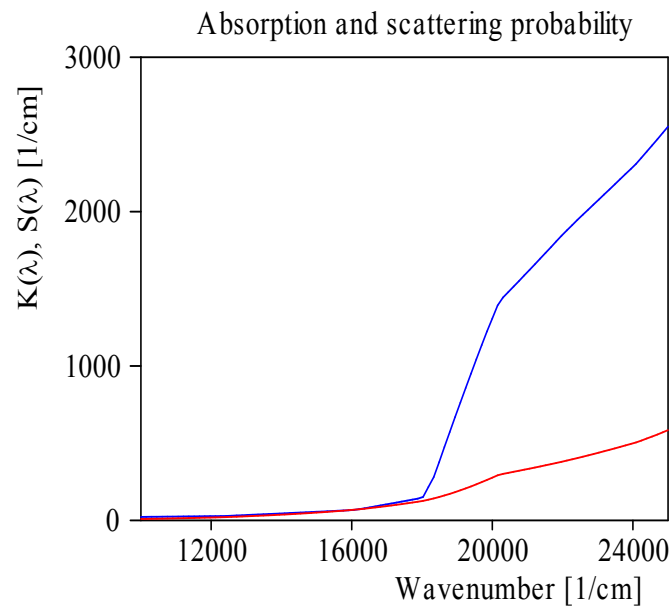
4.2.3 The test system

The paint test system consists of a circular light source (transparent) sending a parallel beam towards the air-resin interface (rectangular, 2 mm * 2 mm). Below this interface there is another one representing the resin-substrate transition. A view of this configuration is given below:
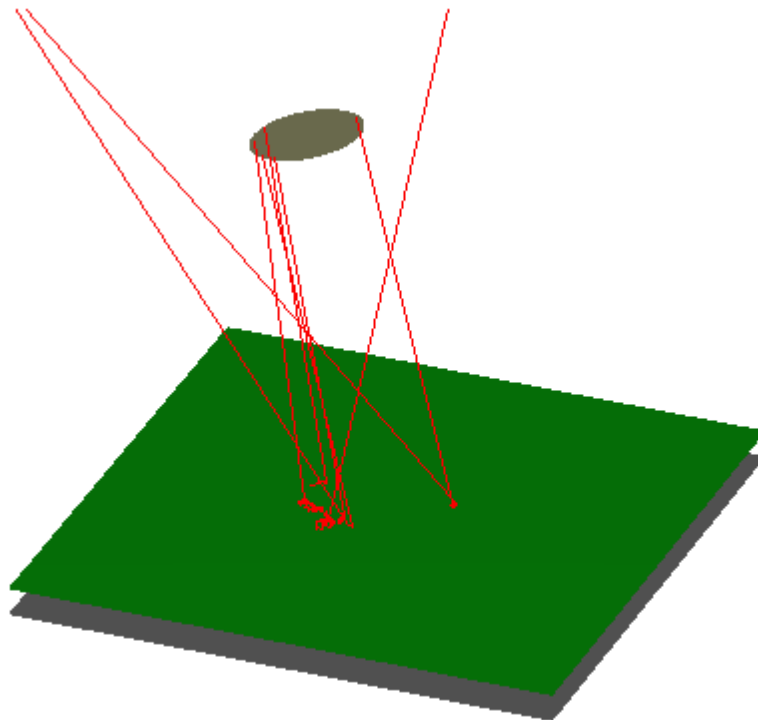

Here is a side view of the arrangement:
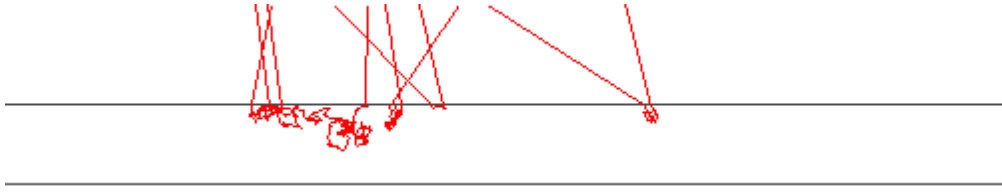
The space between top and bottom interface is filled with a composite scatterer (the TiO_2 and CdS particles). The distance between the interfaces, i.e. the thickness of the paint, is 100 microns. The concentration of the TiO_2 and CdS particles can be varied in the model, like all other parameters and dimensions.

Four perfect mirrors enclose the scattering volume in order to avoid radiation leaving the test volume (reflecting boundary conditions). The next picture shows the four mirrors which are about to be moved to their final positions:
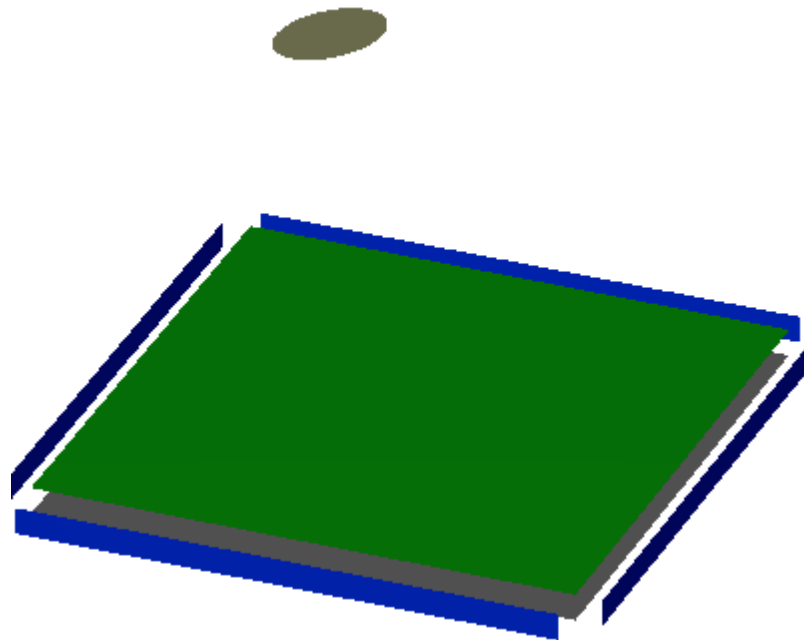
Finally we show the complete system with some test rays:
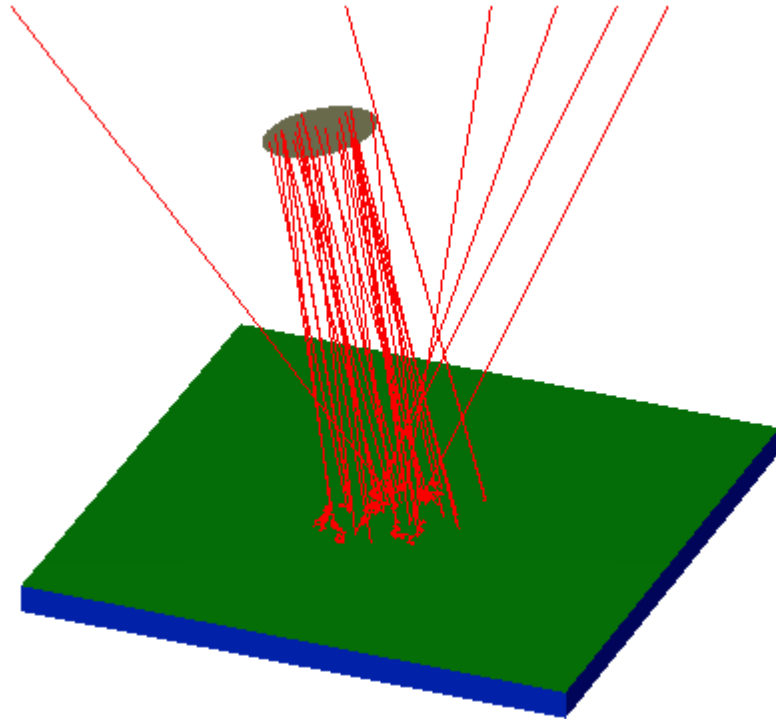
Above the light source there is a huge rectangular detector (10 m * 10 m) collecting all rays that leave the top surface in the upward direction. Since in the views shown above the observer looks downwards the detector is not visible.

4.2.4   Test the test system

Before the actual work begins we should perform some simple tests of the SPRAY setup. This is a very important step since there is a good chance that some of the numerous parameters may be wrong (although we did our best).

No scattering particles, perfect absorber at the bottom interface
Here the rays are partly reflected at the air-resin interface. Since the resin has a constant and real refractive index of 1.5 the reflectance of the top interface is about 4%. All rays transmitted to the bottom interface are absorbed if we use a perfect absorber for that interface. Here is a side view with some test rays:
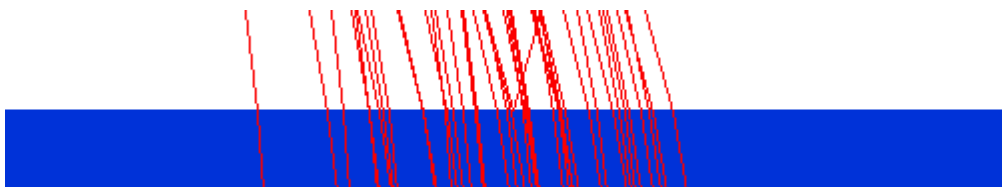

The detector should have a constant signal of about 4%. Doing the simulation in the spectral range 300 ... 1000 nm with 20 spectral points and 10000 rays/spectral point one gets the following detector signal:

Rectangular Detector
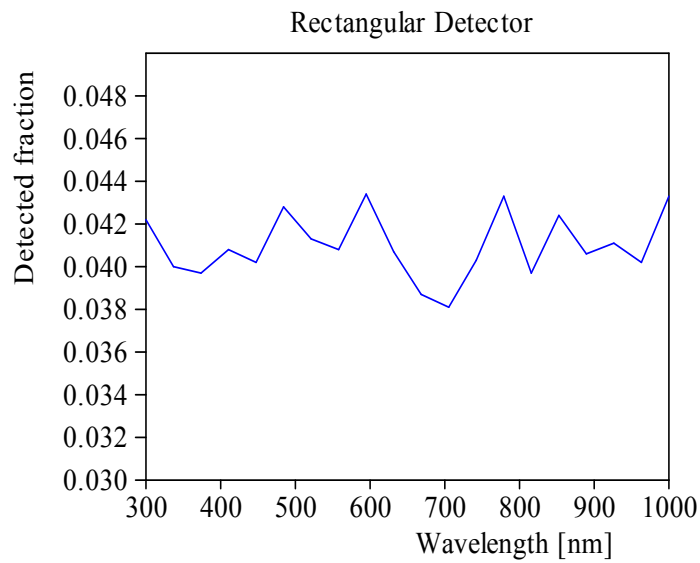
This is the expected behaviour. The noise level can be estimated the following way: If 10000 rays are processed and 4% reach the detector, the average number of rays is 400. The statistical variation of the number of detected rays is the square root of 400, i.e. 20. The amplitude of the noise is then given by (420-380)/10000 = 0.4% which is roughly what you see in the graph above.

No scattering particles, perfect mirror at the bottom interface
In this case all rays are reflected at the bottom interface
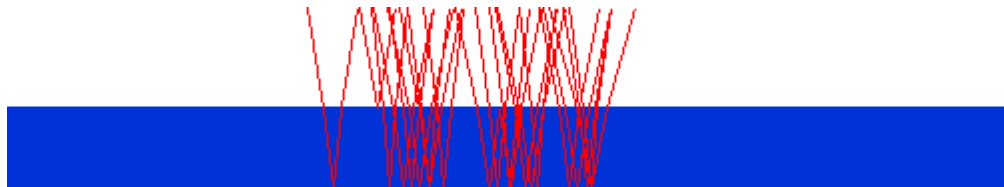
and should reach the detector. We get this:

Rectangular Detector
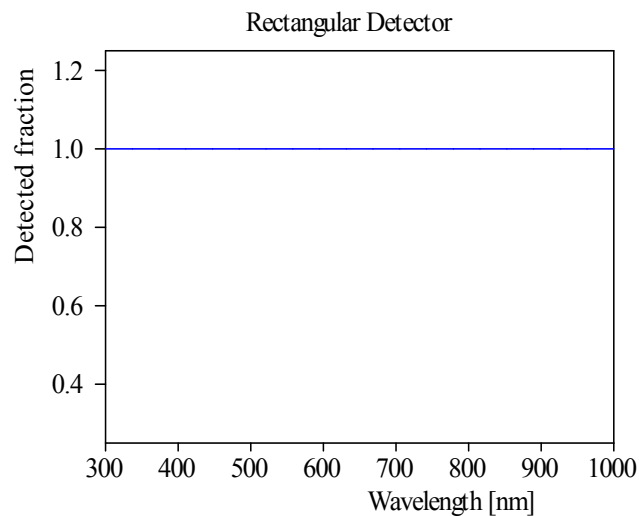
No scattering particles, gold mirror at the bottom interface

This case is used to test a case with spectral variation. The optical constants of gold are taken from the SPRAY database. The obtained spectrum (300 ... 1000 nm, 71 points, 1000 rays/ point) and the corresponding color are shown below:
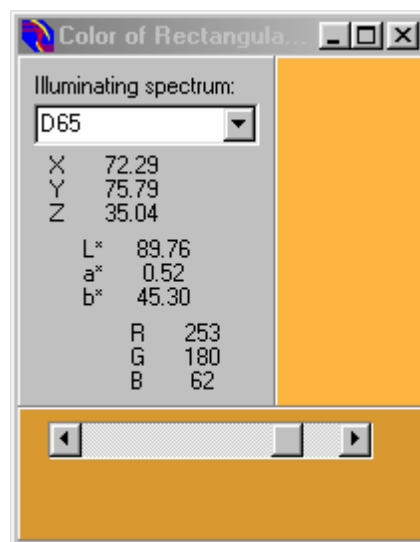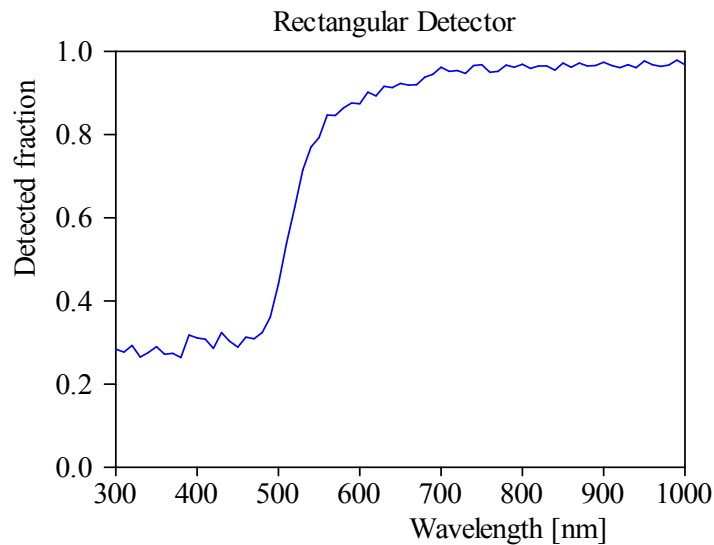

This looks like gold, and we can continue with more serious investigations.

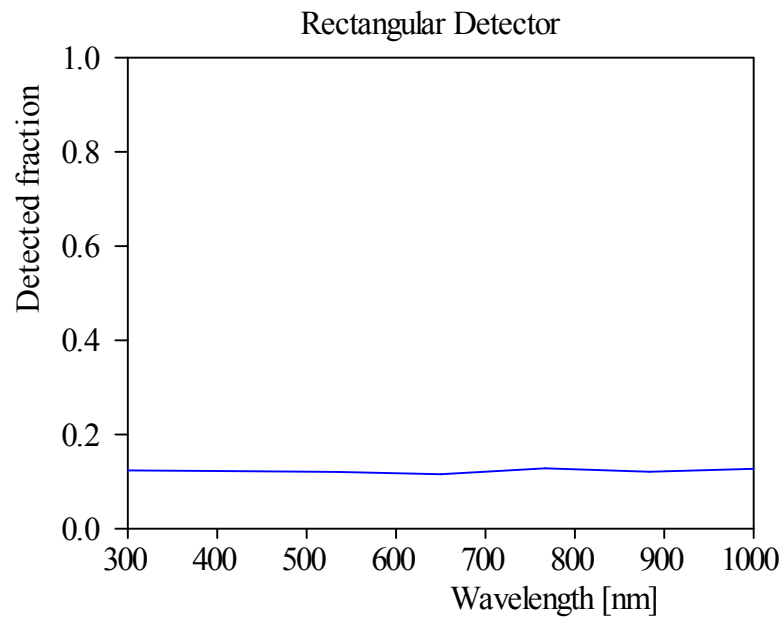## 4.2.5   Large TiO2 particles in resin

Now we can start to look at light scattering. In this first investigation we want to find out how many of the large TiO2 particles we have to add to the paint to make it optically dense, i.e. independent of the substrate.
The bottom interface is set to be a perfect absorber again. As shown in the tests before, the detector signal is 4% (due to the specular reflectance of the air-resin interface) if the volume fraction of the TiO2 spheres is 0. We now slowly increase the volume fraction, compute spectra in the range 300 ... 1000 nm with 7 points (we do not need spectral resolution in this case) and collect the results with the Collect program.
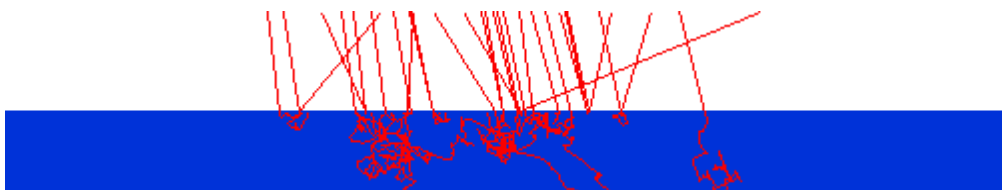
Starting at a volume fraction f = 0.01 a side view shows what happens:
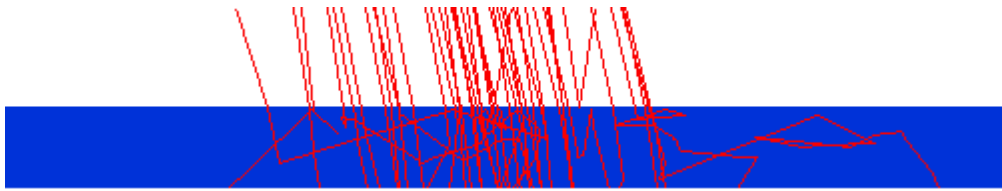
The rays travel through the whole resin layer. Due to the pronounced forward scattering many of the rays that get scattered nevertheless reach the absorbing bottom. Consequently the detector signal is not too high yet:
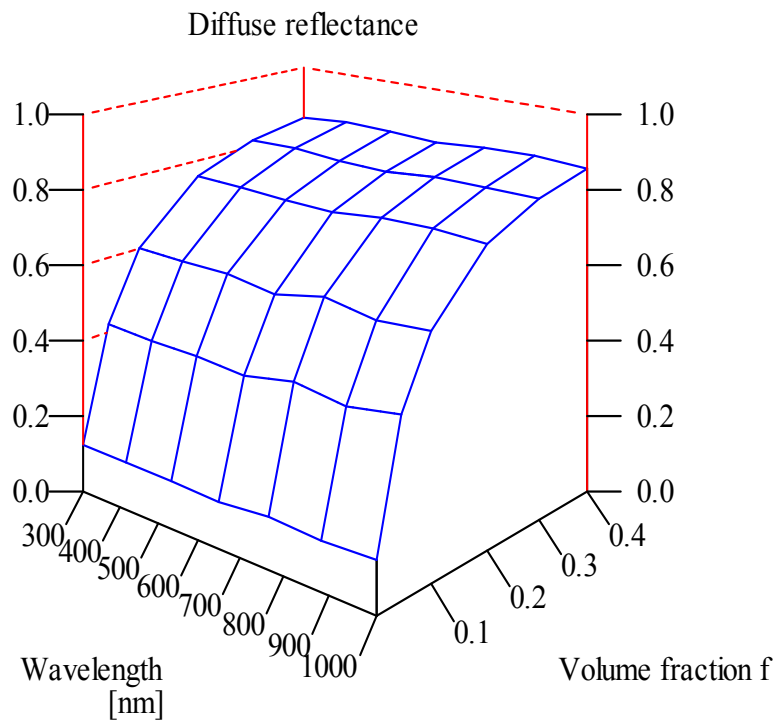
At f = 0.2 almost no particles reach the bottom interface:

The diffuse reflectance signal is much higher now:

Rectangular Detector
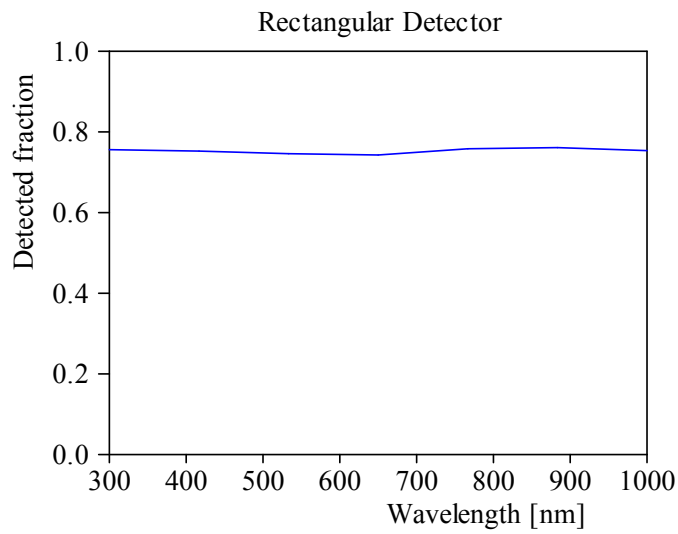
The next graph summarizes the results for various volume fractions:
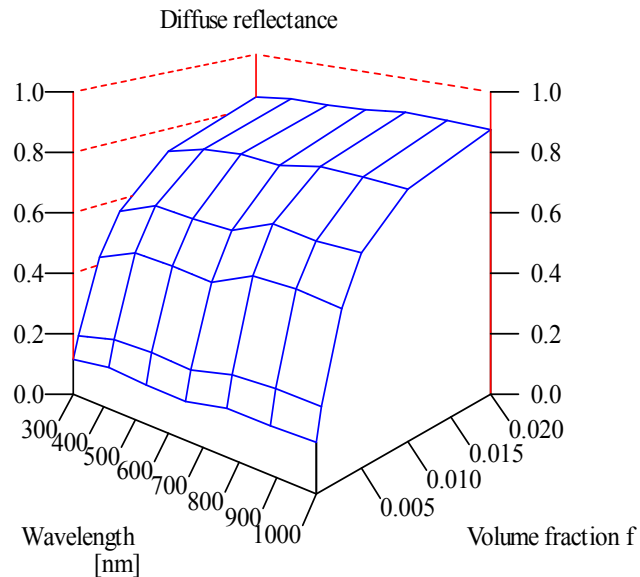
Diffuse reflectance

4.2.6   Small TiO2 particles in resin

To investigate the influence of the TiO2 particle size on the paint performance we repeat the previous computations for the small TiO2 spheres. Here is side view for f = 0.02:
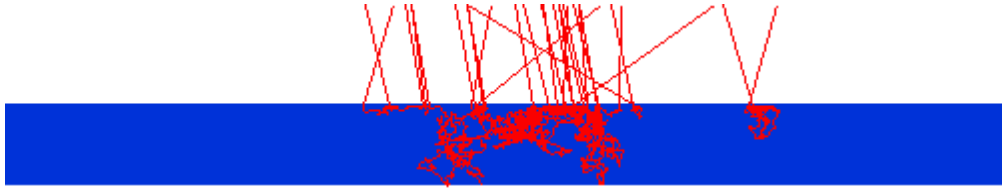
It turns out that much smaller volume fractions are needed to obtain an optically thick paint:


4.2.7   Color by CdS clusters

Finally we add some absorbers to the paint to get a real color. As shown above, the small CdS inclusions absorb in the blue much more than in the red - hence we can expect a color like red, orange or yellow.

Mixing a paint with $f = 0.02$ of the small TiO2 particles and $f = 0.001$ of CdS clusters, the following spectrum (71 points covering the range 300 ... 1000 nm with 1000 rays/point) is obtained:

Rectangular Detector
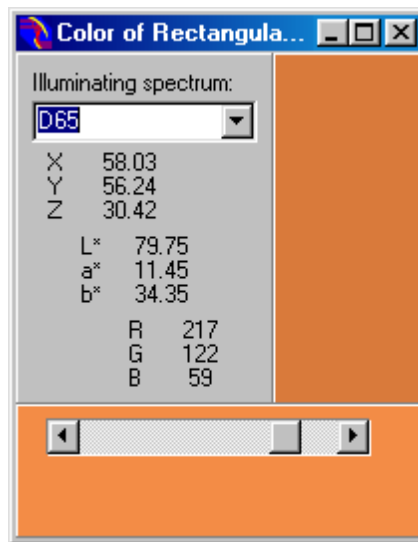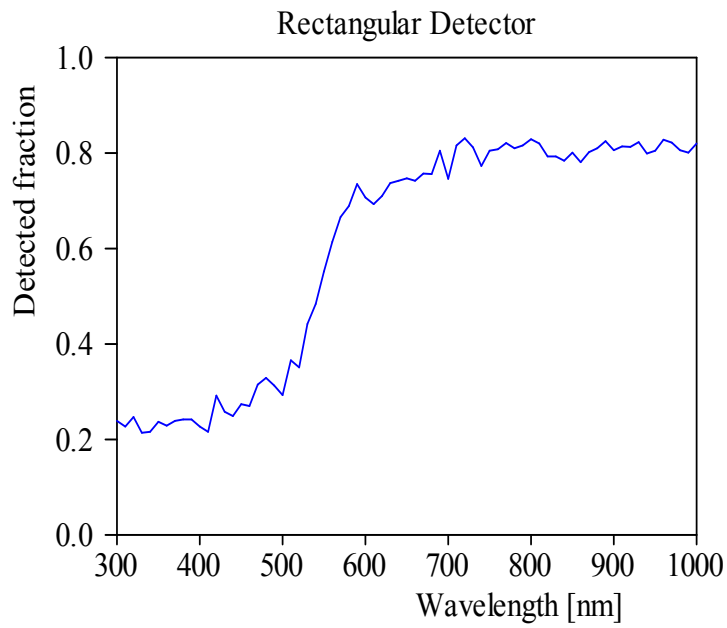
To visulasize what happens we can compare the fate of some test rays for different wavelengths. At 400 nm (blue light) most of the rays get absorbed on their way through the paint:
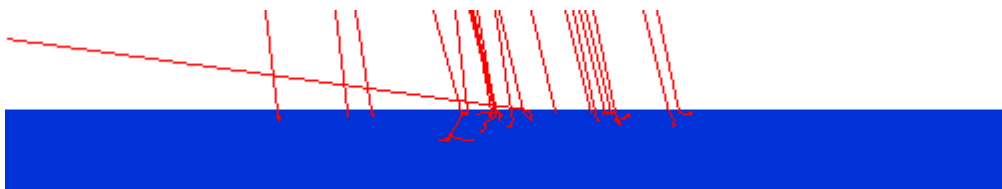
On the other hand, red light (700 nm) can travel much longer through the resin and has a much larger chance to get to the top again without absorption:
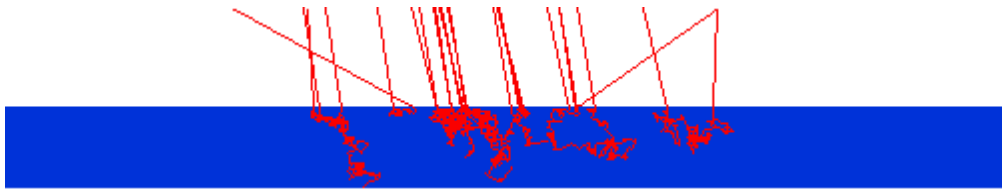
The graph below summarizes the results of various simulations: